Bioresource Technology 124 (2012) 259–268

Contents lists available at SciVerse ScienceDirect

Bioresource Technology

journal homepage: www.elsevier.com/locate/biortech

Towards thermal design optimization of tubular digesters in cold climates: A heat transfer model

Thibault Perrigault [a], Vergil Weatherford [b], Jaime Martí-Herrero [a,*], Davide Poggio [c]

[a] Centre Internacional de Mètodes Numèrics en Enginyeria (CIMNE), Building Energy and Environment Group, Barcelona, Spain
[b] Building Systems Engineering, University of Colorado – Boulder, CO, USA
[c] Instituto para una Alternativa Agraria (IAA) – Cusco, Peru

HIGHLIGHTS

- Low-cost tubular digester are developed for cold climate.
- Thermal performance was analyzed by exhaustive temperature monitoring.
- A one-dimensional, time-dependent heat transfer model was developed.
- Solar gains, influent/effluent flows, ground temperature impact are considered.
- The model agrees with experimental within ±0.47 °C for slurry temperature.

ARTICLE INFO

Article history:
Received 14 June 2012
Received in revised form 2 August 2012
Accepted 6 August 2012
Available online 14 August 2012

Keywords:
Anaerobic digestion
Plug flow
Low-cost tubular digester
Thermal performance
Heat transfer

ABSTRACT

A cold climate, low cost, tubular digester is monitored and temperatures from different parts of the slurry, greenhouse, and adobe walls are presented, discussing the thermal performance of the digester. The slurry exhibits a vertical gradient of 6 °C, with a mean value of 24.5 °C, while the ambient temperature varies from 10 °C to 30 °C, showing the efficiency of the system as a solar heat collector with thermal inertia. A simple time-dependent thermal model is developed using inputs of solar radiation, wind velocity, ambient temperature, and digester geometry. The model outputs include temperatures of the slurry, the biogas, its holding membrane and the greenhouse air, wall and cover. Radiative, convective and conductive heat transfer phenomena are considered between all system elements. The model has 0.47 °C (2%) standard error for the average slurry temperature. This model can be used to predict the influence of geometry and materials on the performance of the digester.

1. Introduction

Anaerobic digestion (AD) of manure is a promising technology that provides both a clean energy source (biogas) and an enriched fertilizer while also improving environmental sanitation. These benefits make anaerobic digestion particularly suitable as a decentralized energy source for remote rural areas (Preston and Rodríguez, 2002; Velo, 2006).

The uses and benefits of AD at the household scale have been widely demonstrated in China and India where several million small-scale biogas plants have been installed over the last few decades and also—more recently—in Nepal (Bhattacharya and Jana, 2009; Gautam et al., 2009; Yu et al., 2008; Zhang et al., 2009). The digester models built have been predominantly fixed-dome (Chinese model) and floating-dome (Indian model) digesters usually constructed from brick masonry (Liming, 2009). However, without funding, the high labor and materials costs for these types of digesters usually prohibits the average farmer from building them. A cheaper and more easily constructed anaerobic digester is the plug-flow plastic tubular digester (PTD) (Botero and Preston, 1987), also known as the low-cost tubular digester, and construction costs are typically within reach of the small farmer.

In such plug-flow reactors, wastewater flows horizontally from one end to the other in a trench lined with tubular polyethylene or PVC sheeting, while biogas is collected from the headspace of the "bag" by means of a gas pipe connected to a reservoir (Ferrer et al., 2011).

Anaerobic digestion is a temperature sensitive process: average operating temperature affects the reaction rates of the process (Bohn et al., 2007), while temperature fluctuations can affect its stability (Alvarez and Liden, 2008). Traditionally, PTD digesters

* Corresponding author. Address: Centre Internacional de Mètodes Numèrics en Enginyeria (CIMNE), Building Energy and Environment Group, C/Dr. Ulles, 2, 3, 08224, Terrassa (Barcelona), Spain. Tel.: +34 937899169; fax: +34 937883110.
E-mail address: jaimemarti@cimne.upc (J. Martí-Herrero).

0960-8524/$ - see front matter © 2012 Elsevier Ltd. All rights reserved.
http://dx.doi.org/10.1016/j.biortech.2012.08.019

Nomenclature

A	area [m^2]
C_p	specific heat capacity [J/kg K]
D	damping depth [m]
E	width [m]
F	shadow factor [.]
F	radiative view factor [.]
h_r	radiative heat transfer coefficient [W/m^2 K]
h_c	convective heat transfer coefficient [W/m^2 K]
h_{wind}	heat transfer coefficient due to wind [W/m^2 K]
I	irradiation (instantaneous radiation) [W/m^2]
k	thermal conductivity [W/m K]
L	characteristic length [m]
m	mass [kg]
N_{u_L}	Nusselt number [.]
Pr	Prandtl number [.]
Q_r	radiative heat gain (or loss) [W]
Q_c	convective heat gain (or loss) [W]
Q_{cd}	conductive heat gain (or loss) [W]
Q_{wind}	heat loss due to wind [W]
Ra	Rayleigh number [.]
Re	Reynolds number [.]
S	solar insolation (radiation over time) [W]
Z	depth [m]
T	temperature [K]
U	velocity [W]
α	absorbance for *gc*, *w1*, *w2*, *gh* and *s*; thermal diffusivity for *air*, *ga* and *g* [–] ; [m^2/s]
τ	transmissivity [–]
ε	emissivity [–]
β	volumetric thermal expansion coefficient (1/T) [K^{-1}]
Ω	inclination angle [°]
σ	Stefen–Boltzmann constant [W/m^2 K^4]
ν	kinematic viscosity [m^2/s]
ρ	density [kg/m^3]
μ	dynamic viscosity [Pa s]

Subscripts

air	air
amt	ambient
ext	external
in	inlet feeding
ins	insulation
int	internal
g	biogas
ga	greenhouse air
gc	greenhouse cover
gh	gas holder
gr	ground
s	slurry
sky	sky
w1	wall 1
w2	wall 2

are built in tropical climates, where the average ambient temperature is favorable to the anaerobic digestion process (Lansing et al., 2010; Sarwatt et al.,1995), whereas low-cost digesters built in rural mountain areas, such as the Bolivian and Peruvian *Altiplano* must be able to function given low and fluctuating ambient temperatures.

The *Altiplano,* at an elevation from 3000 to 4000 m above sea level (m.a.s.l.), is swept by strong winds, and has an arid, cold climate with large diurnal temperature swings. The average daily highs range from 15 °C to 20 °C and the average lows from −15 °C to 3 °C with an atmospheric pressure around 60–70 kPa and an elevated mean solar radiation of 5.5 kWh/(m^2 day) (Alvarez and Liden, 2008).

Due to the cold climate conditions of the *Altiplano*, the cost-effectiveness of biogas production depends on maintaining a digester slurry temperature higher than the average ambient temperature. Several methods for increasing the digester temperature have been proposed in the literature: mixing the input feedstock material with hot water, building an aerobic compost pit around the digester and enclosing the biogas plant inside a greenhouse or 'solar canopy' (Kishore, 1989).

A new concept of a low-cost greenhouse-integrated PTD was developed specifically for the climatic conditions of the *Altiplano* (Martí-Herrero, 2007, 2008, 2012; Poggio, 2007). In this arrangement, the tubular digester is insulated from the ground and integrated into a greenhouse composed of thermally massive adobe walls and covered with a transparent plastic sheet. Adobe walls store heat during the day and release it at night. Preliminary reports on the implementation of this technology underline the impacts on biogas production rate due to the operating temperature (Poggio et al., 2009), the geometric design of the digester (Martí-Herrero, 2011, 2012) and its organic loading rate (Ferrer et al. 2011).

Particularly, the thermal behavior of PTD in cold climates should be enhanced in order to maximize the average temperature and stabilize the diurnal temperature variations in the reactor. This will result in a more complete conversion of organic matter to biogas allowing a shorter retention time which yields a reduction of system size and cost. It is therefore necessary to understand the mechanisms of thermal coupling of the biogas plant with its surroundings through thermal monitoring and validated mathematical models. There are a few heat transfer models for anaerobic digestion in the literature, but none to date address low cost tubular digesters.

Singh et al. (1985) developed a time-dependent mathematical model to study the effects of including different types of insulation on the inner surface of the gas holder of a fixed dome and floating dome type digesters. The model assumed that the majority of heat transfer occurs between the top of the dome and the ambient air and that the heat transfer is one dimensional. Kishore (1989) carried out a steady-state heat transfer analysis for fixed-dome biogas plants. The analysis takes into account heat losses from the surface of the slurry inside the digester as well as the heat losses to the surrounding earth (conduction, thermal radiation and convection). The investigation focused on the effects of several thermal improvement suggestions. Usmani et al. (1996) developed an analytical expression, based on climatic data, for the instantaneous thermal efficiency of a greenhouse-integrated above ground biogas system (floating dome type) and the instantaneous thermal loss efficiency factor from the system for a given capacity. Gebremedhin et al. (2005) developed a mathematical model that predicts the energy requirements to operate a heated plug-flow anaerobic digester at a specified temperature. The model accounts for heat loss/gain by the influent and effluent flows, the digester floor, top-covering material and walls. Also, the model accounts for frozen ground surrounding digester walls. A weather and ambient temperature model is introduced. Chen (2007) pursued a sensitivity analysis based on this model.

Other reports deal with active solar anaerobic reactor systems. Axaopoulos et al. (2001) investigated a solar heated system that

consisted of a digester covered with flat-plate solar collectors connected to a heat exchanger immersed in the slurry. El-Mashad et al. (2004) studied two different types of completely stirred, thermophilic, anaerobic reactor systems. One system consisted of a solar collector placed outside of the reactor, and the other with a solar collector mounted on the reactor roof. The experimental investigations focused on the effects of temperature fluctuations, reactor size, and insulation characteristics on methane production. These kinds of active solutions increase the cost and complexity of the digesters and are considered to be less appropriate for small farmers in low income countries.

Garfí et al. (2011) reported some experimental temperature data of a low cost tubular digester at 2800 m.a.s.l. in Cajamarca (Perú) in a greenhouse, showing how the slurry keeps an almost constant temperature around 20 °C, while the greenhouse reaches temperatures of up to 60 °C during the day and 15 °C at night time, with ambient temperature from 10 °C to 30 °C. Garfi et al. conclude that "the effect of the greenhouse on process temperature is doubtful". Ferrer et al. (2011) also reports results of this digester, but does not focus on thermal performance.

The present work, focused on the thermal performance and the heat transfer model for tubular digesters in cold climates, lays the groundwork for the thermal optimization of the digester design. In the future, a parametric analysis that studies the influence of material and geometry of each system component on the thermal performance will provide the rest of the picture. Results for different climates could be shown, as well as recommendations for design strategies that improve the performance of this technology in practice.

This present paper presents an exhaustive temperature monitoring study of an experimental digester in Kayra at 3400 m.a.s.l (Cusco, Peru). Through a 5-day monitored period, several conclusions are presented about the thermal behavior of the cold climate digester system, including the analysis of the heat transfer phenomena that govern this performance. Also, a heat transfer model for low cost tubular digesters is developed, calibrated and validated. The model proposed here is a one-dimensional, time-dependent model for a plug-flow PTD digester in a greenhouse. The model accounts for solar gains as well as heat transfer with the ground, the greenhouse air, the plastic greenhouse cover, the greenhouse walls, the ambient air, and mass transfer via the influent and effluent flows. The model is calibrated and validated with experimental data collected from a low cost digester in the Altiplano of Peru, reaching satisfactory accuracy. This paper is the result of the Perrigault (2009) thesis and Weatherford (2010) masters report, where more detailed analysis can be found.

2. Methods

2.1. Digestion plant

A 2.5 m^3 experimental digester was installed at the *K'ayra* Agronomy Campus, Cusco, at an altitude of 3400 m.a.s.l. The digester was fed daily with a mixture of cow manure and water and operated with a hydraulic retention time of 60 days. The tubular reactor was built of PVC membrane, insulated from the ground with straw and integrated into an adobe and polyethylene sheet plastic greenhouse. The same digester was monitored for gas production in another study (Ferrer et al., 2011), reporting a volumetric productivity and a specific biogas production of 0.47 $m^3\ m^{3-1}\ d^{-1}$ and 0.36 $m^3\ kg^{-1}\ V\ S^{-1}$ respectively.

2.2. Measurements

Meteorological and process data were recorded during 5 days at the end of the rainy summer period (average ambient temperature around 16 °C). Meteorological data included solar radiation, wind speed and direction (at 1.8 m height), relative humidity and ambient temperature. Digester temperatures were monitored in 16 different points (Fig. 1), including 9 sensors inside the digester slurry, soil temperatures at 5 and 70 cm below the surface, air temperature above the slurry, air temperature inside the protective greenhouse, temperatures on both sides of the straw insulation, and on the inside and outside surfaces of the adobe wall. The solar radiation and wind data were collected every 30 s, and temperatures were recorded every minute. The data were then averaged on an hourly basis for consistency and to facilitate importation into the model. Instrument characteristics and specifications are reported in Table 1.

Sensors were installed inside the test digester through the outlet tube. Since the HOBO UA-002 loggers are waterproof and buoyant, they were tied together as 3 sets of 3 strings, weighted, and spaced along a central cord used to facilitate retrieval of the sensors. A ½" PVC pipe served as a semi-rigid guide when inserting the sensors into the outlet tube. Sensors on the surface of the walls were isolated from ambient conditions with small pieces of rigid white foam insulation. Fig. 1 shows the locations of the temperature sensors inside the digester during the verification study.

3. Mathematical model

Assumptions

(1) Each element of the system is represented by a single temperature (1-D);
(2) Heat capacities of the greenhouse cover, air in the greenhouse, digester gas holder and biogas are neglected;
(3) Gas volume inside the gas holder is assumed to be constant and approximated as a rectangular prism calculated for a totally inflated gas holder;
(4) Infrared heat radiation is not absorbed by gases;
(5) Heat losses from evaporation inside the digester and mass flow rate of gas are neglected (Kishore, 1989);
(6) Stratification along the depth of the slurry, the gas column and the greenhouse inside air are neglected;
(7) Inward and outward greenhouse air infiltrations are neglected;
(8) Greenhouse cover transmissivity is independent of the direction of the incident solar radiation;
(9) Reflected solar radiation inside the system is neglected;
(10) It is assumed that microbial heat generation is negligible. Hashimoto and Chen (1979) showed that heat gain from the exothermic reaction can be neglected;
(11) Properties of the feeding mixture added to the system are assumed to be equivalent to the properties of the slurry with the exception of temperature, which is equal to ambient temperature;
(12) Heat loss through the small end-wall is neglected as are losses at the entrance and exit tubes;
(13) Uniform soil properties (specific heat, thermal conductivity and density) are assumed throughout the depth;
(14) At all depths, soil temperature varies sinusoidally with the same annual frequency around an average value. At increasing depths, temperatures oscillates with decreasing amplitudes and increasing phase lags (Hillel, 1982);
(15) It is assumed that digester does not affect the soil temperature and the temperature of the soil remains the same regardless of the digester temperature (Hills,1986);

3.1. Energy balances

The proposed model is built through the energy balance of each element identified in Fig 2.

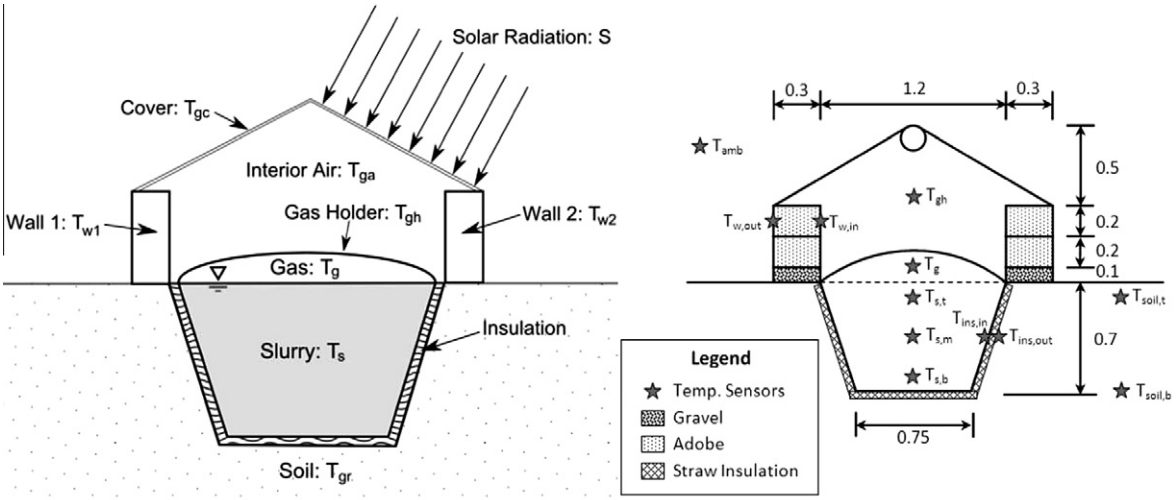

Fig. 1. General cross-section of the digester simulated in the 1-D thermal computer model and locations of the temperature sensors in and around the experimental digester. Length measurements are in meters.

Table 1
Instrument specifications.

Data	Equipment	Resolution	Accuracy
Solar radiation	Pyranometer – Eko MS-602 w/ HOBO U12 logger	0.37 W/m^2	±5%
Windspeed	Davis standard anemometer w/ HOBO U12 logger	0.1 m/s	±1 m/s
Ambient, soil temp/RH	HOBO U12-013 logger with 2 ext. temp probes	0.03 °C/0.03%	±0.4 °C/±2.5%
Air and slurry temps	HOBO UA-002-64 waterproof pendant loggers	0.1 °C	±0.47 °C
Surface temps	HOBO UA-002-64 logger with styrofoam cover	0.1 °C	±0.47 °C

For the greenhouse cover (gc), greenhouse air (ga), wall 1 (w1) and 2 (w2), digester gas holder (gh), gas (g) and slurry (s), the energy balances are expressed, respectively, as:

$$0 = S_{gc} + Q_{r,w1-gc} + Q_{r,w2-gc} + Q_{r,gh-gc} + Q_{r,gc-sky} + Q_{wind,gc} + Q_{c,ga-gc} \quad (1)$$

$$0 = Q_{c,gc-ga} + Q_{c,w1-ga} + Q_{c,w2-ga} + Q_{c,gh-ga} \quad (2)$$

$$m_{w1}C_{p,w1}\frac{\partial T_{w1}}{\partial t} = S_{w1} + Q_{r,w1-sky} + Q_{r,gc-w1} + Q_{r,w2-w1} + Q_{r,gh-w1} + Q_{c,w1-ga} + Q_{wind,w1} \quad (3)$$

$$m_{w2}C_{p,w2}\frac{\partial T_{w2}}{\partial t} = S_{w2} + Q_{r,w2-sky} + Q_{r,gc-w2} + Q_{r,w1-w2} + Q_{r,gh-w2} + Q_{c,w2-ga} + Q_{wind,w2} \quad (4)$$

$$0 = S_{gh} + Q_{c,gh-s} + Q_{c,gh-ga} + Q_{r,gh-w1} + Q_{r,gh-w2} + Q_{r,gh-s} + Q_{r,gh-gc} \quad (5)$$

$$T_g = (T_{gh} + T_s)/2 \quad (6)$$

$$m_s C_p, s\frac{\partial T_s}{\partial t} = S_s + Q_{c,s-gh} + Q_{r,gh-s} + Q_{cd,s-gr} + Q_{in} \quad (7)$$

3.2. Radiative heat transfer to the sky

The sky is assumed to be a black body at the temperature equivalent to (Swinbank, 1963):

$$T_{sky} = 0.0552T_{amb}^{1.5} \quad (8)$$

The radiative heat transfer from the greenhouse cover and the walls to the sky may be obtained, with the view factor $f_i = (1 + \cos(\omega_i))/2$ and $i \in \{gc, w1, w2\}$ from (Duffie and Beckman, 1980):

$$Q_{r,i-sky} = \sigma f_i \epsilon_i A_i (T_i + T_{sky})\left(T - i^2 + T_{sky}^2\right)(T_i - T_{sky}) \quad (9)$$

3.3. Radiative heat transfer between digester elements

The radiative heat transfer from one element of the system to another one is expressed as (Duffie and Beckman, 1980):

$$Q_{r,i-j} = \sigma A_i \frac{(T_j^2 + T_i^2)(T_j + T_i)}{(1-\epsilon_j)A_i/\epsilon_j A_j + 1/f_{i-j} + (1-\epsilon_i)/\epsilon_i}(T_i - T_j) \quad (10)$$

With $(i,j) \in \{gc,w1,w2,gh\}$ or $(i,j) \in \{s,gh\}$. $(f_{i,j})$ is the view factor from the element "i" to the element "j".

3.4. Convective heat transfer to the ambient air

The convective heat transfer between an element of the greenhouse (cover and walls) and the ambient air is expressed, with $i \in \{gc,w1,w2\}$:

$$Q_{wind,i} = h_{wind,i}A_i(T_i - T_{amb}) \quad (11)$$

Datta (2002), treated the digester as a flat plate and calculate the convective heat transfer coefficient of air (h_{wind}) from the Nusselt Number (Nu)

$$N_{u_L} = h_{wind}L/k_{air} = \left\{\begin{array}{ll} 0.664Re^{1/2}Pr^{1/3} & Re < 2\times10^5 \\ 0.037Re^{4/5}Pr^{1/3} & Re > 3\times10^6 \end{array}\right\} \quad (12)$$

$$Re = U_{wind}L/\nu_{air} = \rho_{air}U_{wind}L/\mu_{air} \quad (13)$$

3.5. Convective heat transfer in the greenhouse

The greenhouse air can gain or lose heat by free convection by the two walls, the greenhouse cover and the gas holder. Calculations of the Nusselt Number in those cases depend only on heat

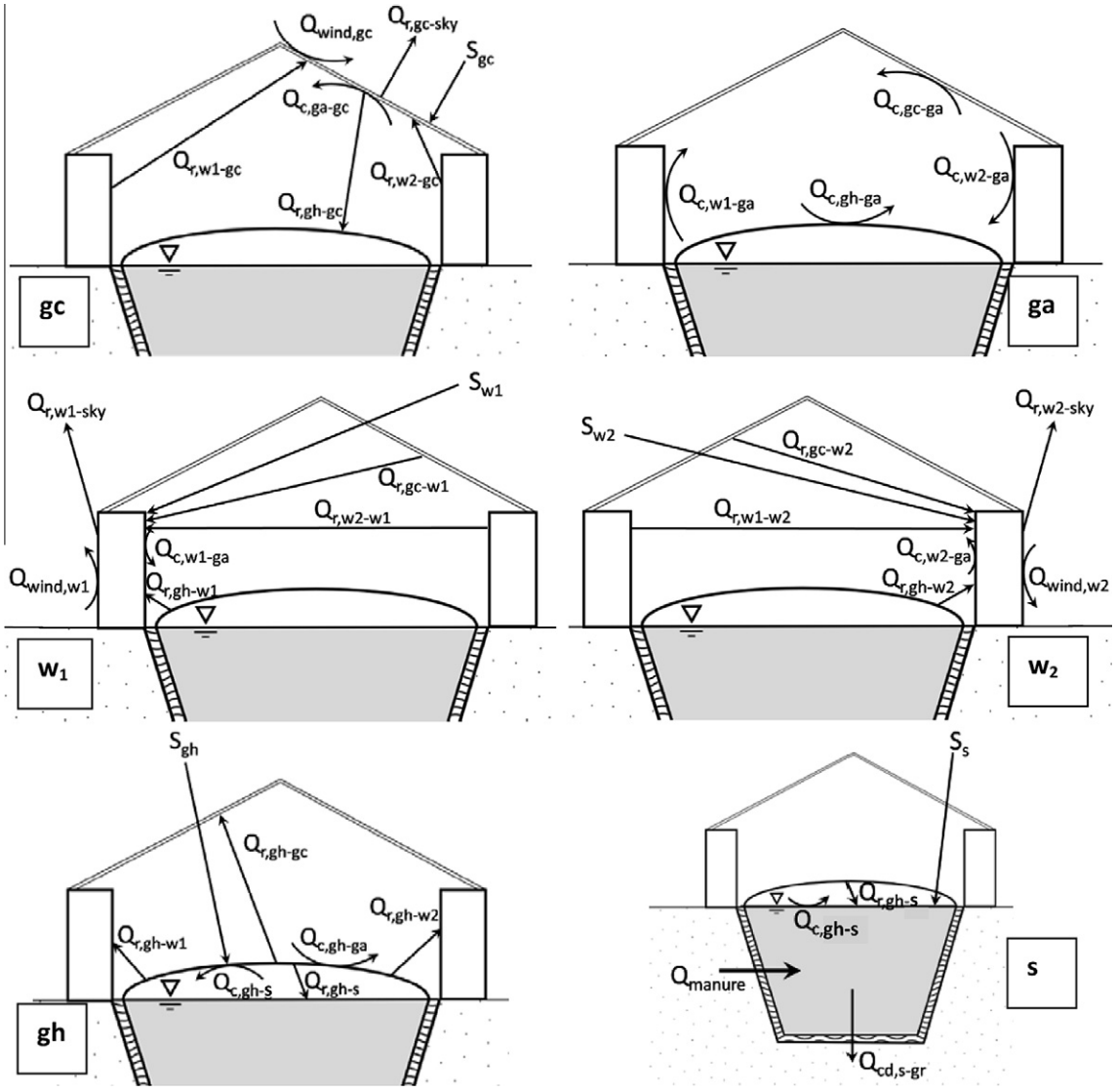

Fig. 2. Detailed scheme of the heat transfer phenomena considered for each element of the digester.

transfer area orientation (in this study: horizontal for *gh*; vertical for *w1* and *w2*; and tilted for *gc*) and the fluid/solid temperature difference:

$$Q_{c,i-ga} = h_{c,i-ga} A_i (T_i - T_{ga}) \tag{14}$$

With $i \in \{gc, w1, w2, gh\}$. All convective heat transfer coefficient calculations are based on the Nusselt and Rayleigh Numbers calculations:

$$h_{c,i-ga} = N_{u_L} \cdot k_{ga}/L \tag{15}$$

$$R_{a_L} = g\beta_{ga}(T_i - T_{ga})L^3/\alpha_{ga}\nu_{ga} \tag{16}$$

For vertical plates, the characteristic length (L) is the plate height (Incropera and Dewitt, 1996):

$$N_{u_L} = \begin{Bmatrix} 0.68 + \left(0.67R_{aL}^{1/4}\right)/\left(1 + (0.492/Pr)^{9/16}\right)^{4/9} & R_{aL} \leqslant 10^9 \\ \left(0.825 + \left(0.387R_{aL}^{1/6}\right)/\left(1 + (0.492/Pr)^{9/16}\right)^{8/27}\right)^2 & R_{aL} \geqslant 10^9 \end{Bmatrix} \tag{17}$$

For horizontal plates, the characteristic length (L) is the ratio between the plate area and perimeter. For an upper surface of hot plate or lower surface of cold plate, Nusselt Number is expressed as (Incropera and Dewitt, 1996):

$$N_{u_L} = \begin{Bmatrix} 0.54R_{aL}^{1/4} & 10^4 \leqslant R_{aL} \leqslant 10^7 \\ 0.15R_{aL}^{1/3} & 10^7 \leqslant R_{aL} \leqslant 10^11 \end{Bmatrix} \tag{18}$$

and for the lower surface of a hot plate or the upper surface of cold plate (Incropera and Dewitt, 1996):

$$N_{u_L} = 0.27R_{a_L}^{1/4} \quad 10^5 \leqslant R_{a_L} \leqslant 10^{10} \tag{19}$$

For inclined plates: the inclination angle (θ) refers to the angle from vertical, in the case $0 \leqslant \theta \leqslant 60°$ and for the lower surface of a hot plate or the upper surface of a cold plate, the calculations are the same as for a vertical plate except that the Rayleigh number is calculated substituting g for $g\cdot\cos(\theta)$ on Eq. (16). The characteristic length is equal to the plate width. In all the others cases where $\theta \leqslant 60°$ the vertical plate calculation is used and for $\theta > 60°$ the horizontal plate calculation is used.

3.6. Convective heat transfer in the gas holder

The biogas contained in the gas holder can gain or lose heat by convection with the gas holder and the slurry. To calculate it, we consider the gas holder as a horizontal rectangular cavity, with the upper and lower surfaces (gas holder and slurry) at different

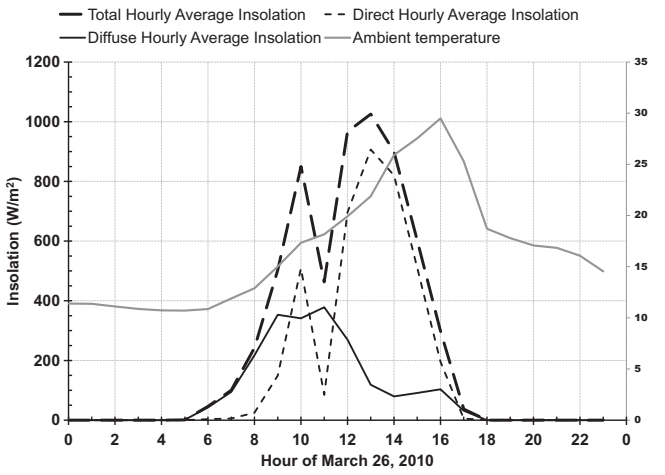

Fig. 3. Direct, diffuse, and total horizontal radiation for a typical day during the study period. The secondary axis refers to ambient temperature.

temperatures while the remaining surfaces are assumed to be insulated from the surroundings (Incropera and Dewitt, 1996).

$$Q_{c,s-gh} = h_{c,s-gh} A_i (T_s - T_{gh}) \tag{20}$$

$$R_{a_L} = g\beta_g (T_s - T_{gh}) L^3 / \alpha_g \nu_g \tag{21}$$

The characteristic length is the average gas thickness in the gasholder. For $T_s > T_{gh}$, the Nusselt Number is expressed as:

$$\left\{ \begin{array}{ll} R_{a_{L_s}} \leqslant 5.10^4 & h = k_m / L N_{u_{L_s}} = 1 \\ 3.10^5 < R_{a_{L_s}} & N_{u_{L_s}} = 0.069^{1/3} Pr_m^{0.074} \end{array} \right\} \tag{22}$$

For $T_s < T_{gh}$, there is no convection but is approximated as conduction.

3.7. Temperature profile through the ground

Hillel (1982) expressed the annual variation of daily average soil temperature at different depths with the following equation:

$$T_{gr}(z,t) = T_{gr,av} + A_0 e^{-z/d} \sin\left[\frac{2\pi}{365}(t - t_0) - \frac{z}{d} - \frac{\pi}{2}\right] \tag{23}$$

where $T_{gr}(z,t)$ is the soil temperature at time t (day) and depth z (m), $T_{gr,av}$ is the average soil temperature of the surface, A_0 is the annual amplitude of the surface soil temperature (°C) calculated as the half of the difference between the maximum mean ambient temperature and minimum mean ambient temperature of one year, d is the damping depth (m) of annual fluctuation expressed as $d = \sqrt{2 \cdot k/(\rho C_p) \cdot 3600 \cdot 2/\omega}$, with $\omega = 2\pi/365$ and t_0 is the time lag (days) from an arbitrary starting date to the occurrence of the minimum temperature in a year. Following the method of Wu and Nofziger (1999), the average soil surface temperature (for an unshaded area) is calculated by increasing the average ambient temperature value by 2°.

3.8. Conduction heat transfer from the slurry to the ground

The slurry inside the digester is contained in a ditch, insulated with straw and covered by a plastic sheet. Conduction between the slurry and the ground is expressed as:

$$Q_{cd,s-gr} = 1 \Big/ \left(\sum k_{ins}/e_{ins}\right) A_{s-gr}(T_s - T_{gr}) \tag{24}$$

Insulation thickness along the ditch sides is different from insulation thickness of the ditch bottom. Moreover, due to the strong dependency of soil temperature on depth, the conductive heat transfer was divided into two parts. The first part is calculated for the ditch bottom using the soil temperature at the ditch bottom depth. The second part is calculated for the ditch sides using a lateral ground temperature equal to the mean temperature between the soil surface and the digester base. Both ground temperatures are calculated using Eq. (23).

3.9. Solar radiation heat absorbed

The solar radiation heat flux absorbed by the greenhouse cover is given by:

$$S_{gc} = \propto_{gc} \cdot A_{gc} \cdot I_{gc,T} \tag{25}$$

And the solar radiation heat flux absorbed by each wall is:

$$S_{w_1} = \propto_{w_1} \cdot A_{w_1} \cdot (I_{w_1,ext,T} + \tau_{gc} \cdot F_{w_1} \cdot I_{w_1,int,T}) \tag{26}$$

$$S_{w_2} = \propto_{w_2} \cdot A_{w_2} \cdot (I_{w_2,ext,T} + \tau_{gc} \cdot F_{w_2} \cdot I_{w_2,int,T}) \tag{27}$$

where "ext" subscript is used for the wall side in contact with ambient air, and "int" subscript for the wall side in contact with greenhouse air.

The solar radiation heat flux absorbed by the gas holder and the slurry are:

$$S_{gh} = \tau_{gc} \cdot \propto_{gh} F_{gh} A_{gh} I_{gh,T} \tag{28}$$

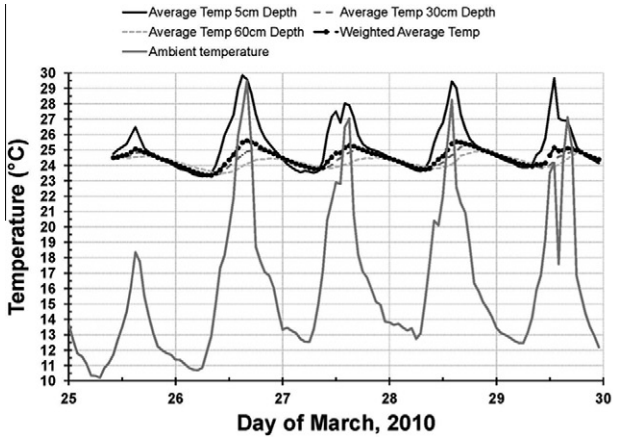

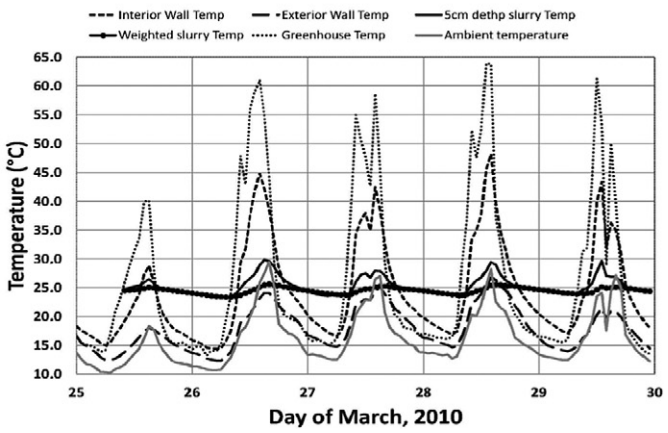

Fig. 4. Left: Experimental average temperature distribution inside the tubular digester, corresponding to 5 cm, 30 cm and 60 cm below the slurry surface and weighted average temperature to characterize the slurry overall. Right: Experimental temperatures of the internal and external surfaces of the adobe greenhouse walls and greenhouse air. The average temperature at 5 cm below the slurry surface, and the slurry weighted average temperature appear as references.

Table 2
Dimensions used in the model.

Digester element	Value
Compacted straw insulation thickness (sides)	5 cm
Compacted straw insulation thickness (bottom)	8 cm
Trench length	5 m
Digester tube diameter	95.5 cm
Digester membrane thickness	2.5 mm
Greenhouse cover thickness	0.5 mm
Orientation from South (West positive)	49°
Mass of daily feedstock (water:manure, 1:1)	40 l
Adobe wall thermal conductivity	1 W/m^2 K
Adobe wall specific heat	835 J/kg K
Straw thermal conductivity	0.32 W/m^2 K
Slurry specific heat	4180 J/kg K
Greenhouse cover visual transmittance	0.65

$$S_s = \tau_{gc} \cdot \cdot \tau_{gh} \cdot \propto_s F_s A_s I_{s,T} \tag{29}$$

F_{w_1}, F_{w_2}, τ_{gh} and F_s are the shading factors. For instance, F_{w_1} describes the percentage of solar radiation striking directly on the inner side of the wall 1 at a given time. Those factors depend on the solar angle and the shading objects' azimuth and height.

3.10. Heat transfer due to mass flow

Every day, the digester is fed with a mass load m_{in}, at one point considered instantaneous, with an inlet stream at temperature T_{in}, which is assumed to be equal to the ambient temperature, an equal amount exits the digester at T_s. The heat transfer due to mass flow can thus be calculated as (Gebremedhin et al., 2005):

$$Q_{in} = m_{in} C_{p,s} (T_{in} - T_s) \tag{30}$$

3.11. Solving algorithm

In order to solve the energy balance equations of the elements with inertia, the following approximation for the partial derivatives is used, substituting them for the corresponding finite differences:

$$\frac{\partial T_i}{\partial t} = \frac{T_i(t + \Delta t) - T_i(t)}{\Delta t} = \frac{T_i^{n+1} - T_{p_i}^n}{\Delta t} \tag{31}$$

With $i \in \{s, w1, w2\}$, Δt = 1 h and "n" a given hour.

The solving algorithm has been written in Matlab, and is as follows:

1. Input all required information (digester dimensions, materials properties, and weather conditions)
2. Assume T_s, T_{w1}, T_{w2} for time n = 1
3. Iterate to get T_{gc}, T_{gh}, T_{ga}, T_g at time n = 1 using Eqs. 1, 2, 5, 6
4. CalculateT_s, T_{w1}, T_{w2} for time n + 1 with Eqs. 3, 4, 7
5. Repeat this procedure from step 3.

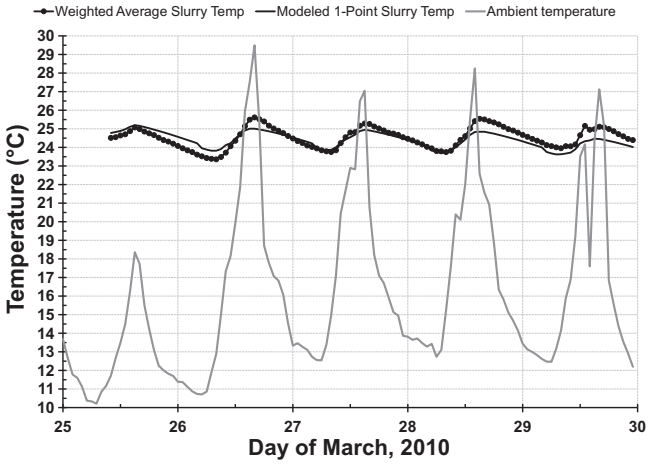

Fig. 5. Modeled and weighted average slurry temperature.

Table 4
Radiative heat transfer parameters used in the model. Note that the Gas holder has τ_{gh} = 0, so S_s is 0 (Eq. (29)) for this case.

Material	Absorbance α	Emissivity ε	Transmissivity τ
Adobe (w1,w2)	0.8	0.8	0
Greenhouse cover (gc)	0.2	0.2	0.65
Geomembrane PVC (gh)	0.8	0.8	0
Slurry (s)	0.8	0.8	0

The model is run for 365 days with weather data from METEONORM, when no measurements exist, and with 21 days of real local weather measurements, including the five days selected for validation to account for the temperature of thermally massive elements.

4. Results and discussions

4.1. Experimental data

Radiation data collected was total global horizontal. In order to calculate the diffuse and direct components, the Boland–Ridley–Lauret (BRL) model was used which, according to a recent study, has a higher correlation for hourly data than other models due to the fact that it accounts for dynamics (sun angle) and persistence effects (Torres et al., 2010; Ridley et al., 2010). In Fig. 3 the direct, diffuse, and total horizontal radiation for an example day during the study period are shown.

The 9 slurry temperatures, arrayed in a 3 × 3 matrix along the length of the digester, were averaged using area-based weighting factors to get the overall temperature of the digester slurry. Because they are closer to heat exchange interfaces, the top and bottom sensors were given weightings equal to the top 10 cm and bottom 10 cm of the slurry. The middle sensor was weighted in relation to the remaining area (45 cm of height). Fig. 4 shows

Table 3
Thermal parameters used in the model.

Material	Density ρ [kg m^{-3}]	Specific heat C_p [J kg^{-1} K^{-1}]	Thermal conductivity k [W m^{-1} k^{-1}]	Thermal diffusivity α [m^2 s^{-1}]	Dynamic viscosity μ [Pa s]	Kinematic Viscosity ν [m^2 s^{-1}]
Adobe and ground (w1, w2, gr)	1450	835	1			
Straw insulation (ins)			0.32			
Slurry (s)	1000	4180				
Ambient air (air, ga)	1.202	1010	$23.94 \cdot 10^{-3}$	$1.972 \cdot 10^{-5}$	$16.9 \cdot 10^{-6}$	$14.06 \cdot 10^{-6}$
Biogas (g)	1.156	1682.2	$25.546 \cdot 10^{-3}$	$16.628 \cdot 10^{-6}$	$11.6 \cdot 10^{-6}$	$11.93 \cdot 10^{-6}$

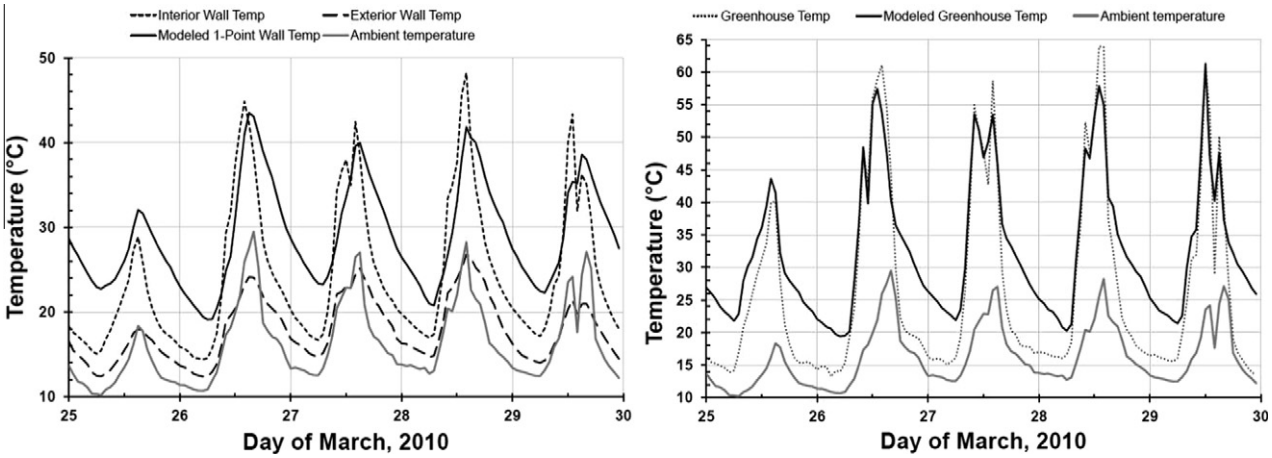

Fig. 6. Left: Modeled and measured wall temperatures. Right: Modeled and measured greenhouse temperatures.

the average of the recorded temperatures at the top, middle and bottom of the slurry, as well as the weighted average temperature. Fig. 4 also shows the temperatures of the interior and exterior wall surfaces, the greenhouse air temperature and the top and weighted average slurry temperatures.

4.2. Analysis of the experimental thermal behavior of the digester

4.2.1. The slurry temperature

According to the experimentally gathered data, the slurry shows a vertical temperature gradient of up to 6 °C. The top of the slurry (as indicated by the 5 cm depth sensor) is influenced by the ambient temperature and solar radiation, with little thermal inertia compared to the rest of the slurry. The temperature of the top layer is consistently higher than the ambient temperature, signifying that solar radiation is the governing heat transfer process for this layer. The sun heats the plastic gas holder, which in turn heats the top of the slurry via radiation and convection through the biogas. The temperature also increases due to the effect of the elevated greenhouse air temperature in contact with the gas holder. Additionally, there exists a heat transfer process from the top layer of the slurry to the lower layers, indicated by an increase in the bottom-layer temperatures during the day. Nighttime temperatures at the top of the slurry drop below those of the lower layers, implying that this layer loses energy to the biogas by convection, to the gas holder by radiation, and to the deeper part of the slurry by convection.

Deeper in the slurry, more thermal inertia is found, with daily amplitudes around 1.5 °C (30 cm depth sensor) and 1 °C (60 cm depth sensor). Average temperatures are around 24.5 °C (at 30 cm) and 24 °C (at 60 cm), while maximum daily temperatures progressively shift to later in the day.

The weighted average temperature accounts for the different temperature profiles in the slurry layers, showing the inertial behavior of the deeper layers and reflecting the quick heating in the mornings due to solar radiation. Over the monitored period, the slurry maintains a mean weighted temperature of 24.5 °C, 8.4 °C higher than the mean ambient temperature (16.1 °C). Garfí et al. (2011) also reported a slurry temperature for a low cost tubular digester in a greenhouse. The ambient temperature conditions during the monitored period reported by Garfi et al. were very similar to those considered in this paper. The mean slurry temperature is about 20 °C in Garfi et al., while the mean ambient temperature is 17.9 °C; a difference of 2.1 °C.

4.2.2. The adobe wall temperatures

The wall temperatures, collected experimentally, give an idea of the influence of the greenhouse. As with the slurry, the walls are massive so the thermal inertia can be seen in their thermal profiles, but high temperature amplitudes are found at the inner surface, due to the heat gain from the warmer air within the greenhouse. Comparing the interior and exterior wall temperatures, there is a difference of 1.5 °C during the night and up to 18 °C during the day. This can only be explained by the effect of the greenhouse, as the sensors are insulated from radiation with foam insulation.

4.2.3. The greenhouse temperature

The greenhouse air temperature had the largest daily amplitude measured: up to 48 °C, with maximum temperatures reaching up to 60 °C. During the night, the greenhouse air temperature fell to values lower than the inner wall surfaces, but still higher than ambient temperature. This means the air inside the greenhouse loses energy to the greenhouse cover, by convection. The cover, in turn, loses heat via radiation to the clear night sky and through convection to the night air, but gains heat from the wall. Garfí et al. (2011) report the temperatures inside a digester greenhouse (with similar conditions to the present study) between 15 to 60 °C, also consistently above the ambient temperature.

4.3. Model calibration and validation

The model was run using the parameters shown in Tables 2–4.The model was calibrated by parametrically adjusting the thickness of the straw insulation by a scaling factor until a minimum standard error is reached for the predicted and the weighted slurry temperature. The thickness of the straw insulation affects the simulation of the slurry temperature in the mean temperature value, but not its daily amplitude. Fig. 5 shows the resulting slurry temperature of the calibrated model with the 9-point weighted average of the experimentally-collected temperatures. Calibrated values of 10 cm along the bottom and 5 cm along the edges yielded results in the minimum standard error between modeled and measured values. The standard error for the predicted slurry T value is 0.47 °C, corresponding to a 2% error with respect to the weighted average experimental temperature of the slurry. The thickness of the straw was measured before the digester installation as 20 cm along the bottom of the ditch and 10 cm along the sides. The calibrated values correspond to 50% of those, which can be assumed to be the compaction of the straw once the digester is filled with liquid.

Fig. 6 shows the modeled wall temperature with the experimentally-collected interior and exterior surface temperatures of the walls. The model appears to over-predict the average wall temperature while it matches the surface temperature on the inside of the wall more closely. This appears to affect the predicted slurry temperature by tempering the nightly low temperatures, causing the model to flatten the temperature peaks and valleys in comparison to the experimental data. The standard error for the predicted wall temperature is 3.08 °C, which corresponds to a 14.6% error with respect to the mean experimental temperature of the wall.

The model tends to predict the temperatures of non-massive elements more closely. For example, Fig. 6 is a comparison of the temperature of the greenhouse air both modeled and experimentally verified. The profiles are very similar in shape, but the modeled temperatures are consistently higher at nighttime. This is related to the over-prediction of the wall temperature and can also be explained by the fact that the model does not consider air infiltration in the greenhouse so the night-time heat losses are lower in the model. The standard error for the predicted greenhouse air temperature is 2.92 °C, corresponding to an 11.1% error with respect the mean experimental temperature.

The proposed model has been calibrated to fit the mean experimental slurry temperature by adjusting the straw insulation thickness. This explains the high correlation between the modeled and experimental slurry temperature, and the higher standard error found in the walls and greenhouse temperatures. The heat transfer phenomena considered in the model describes the system at a basic level, but air infiltration in the greenhouse could be a new parameter to be introduced that could explain the differences between the simulation and real temperature evolution for the greenhouse and walls during night period. This has not been considered due the difficulty of estimating infiltration, which strongly depends on the construction quality of the greenhouse. In order to improve the modeled wall temperatures, a two dimensional heat transfer model could be developed. However, due to the increase in the complexity of the calculations that would be involved, this is beyond of the scope of this work, which seeks to present a simple thermal analysis tool for low cost digesters.

Given very similar ambient conditions and greenhouse performances, the difference in the increase of the slurry temperature over the ambient temperature during the monitored period (8.4 °C for present work, and 2.1 °C for Garfí et al., 2011) can only be explained by the straw insulation. As mentioned before, the amount of insulation affects mean slurry temperature that naturally has very small daily amplitude due to its great thermal inertia. There is no information about the use of insulation on Garfí et al. (2011) or Ferrer et al. (2011), suggesting that none was used. So, 0.05–0.10 m of compacted straw insulation in the ditch may increase the slurry temperature over the mean ambient temperature by as much as a factor of four, compared to having no insulation. Also, the conclusion of Garfi et al. about the "doubtful" effect of the greenhouse on process temperature can be at least partially discredited by the experimental data from the present study showing the elevated temperature of the inner surface of the wall during the nights, indicating that the greenhouse protects the top of the digester from the cool night temperatures, thus reducing heat loss and keeping the slurry warm.

5. Conclusions

The low cost tubular digester has been adapted to cold climates, adding a greenhouse with massive adobe walls, and straw insulation in the ditch. This design acts as a solar heat collector with thermal mass. It gains heat through the cover and, accumulating it in the walls and slurry, reduces heat losses to the ground using straw insulation and to the ambient due the greenhouse. These result in keeping the slurry 8.4 °C above the mean ambient temperature.

This thermal behavior can be simulated by a one dimensional heat transfer model with a standard error of 0.47 °C for the slurry temperature.

Acknowledgements

Financial assistance for this project was provided by the Catalan Development Cooperation Agency (ACCD), the Center for Development Cooperation (CCD) of the Polytechnical University of Catalunya (UPC), the Endev-Bolivia Program of the GIZ, and with the collaboration of the Research Center of Biodigesters, Biogas and Biol (CIB3, Bolivia) and the Caribbean and Latin American Biodigesters Net (RedBioLAC). Thanks to Prof. Arcadio Calderón of the National University of San Antonio Abad of Cuzco (UNSAAC), for helping in the realization of the experimental facility and to Prof. Enric Velo and Prof. Lluis Batet of the Polytechnical University of Catalunya.

References

Alvarez, R., Liden, G., 2008. The effect of temperature variation on biomethanation at high altitude. Bioresource Technology 99, 7278–7284.
Axaopoulos, P., Panagakis, P., Tsavdaris, A., Georgakakis, D., 2001. Simulation and experimental performance of a solar-heated anaerobic digester. Solar Energy 70, 155–164.
Bhattacharya, S.C., Jana, C., 2009. Renewable energy in India: historical developments and prospects. Energy 34, 981–991.
Bohn, I., Bjornsson, L., Mattiasson, B., 2007. Effect of temperature decrease on the microbial population and process performance of a mesophilic anaerobic bioreactor. Environmental Technology 28, 943–952.
Botero, R., Preston, T.R., 1987. Biodigestor de bajo costo para la producción de combustible y fertilizante a partir de excretas: manual para su instalación, operación y utilización. CIPAV, Cali, Colombia. http://www.utafoundation.org/publications/botero&preston.pdf.
Chen, W., 2007. Sensitivity analysis for a plug-flow anaerobic digester. M.S. Thesis. Cornell University, Ithaca, NY. [cited May 2012]. Available from http://hdl.handle.net/1813/8174.
Datta, A., 2002. Biological and Environmental Heat and Mass Transfer. Marcel Dekker, Inc., New York.
Duffie, J.A., Beckman, W., 1980. Solar Engineering of Thermal Processes. John Wiley, John & Sons, New York.
El-Mashad, H.M., van Loon, W.K.P., Zeeman, G., Bot, G.P.A., Lettinga, G., 2004. Design of a solar thermophilic anaerobic reactor for small farms. Biosystems Engineering 87, 345–353.
Ferrer, I., Garfi, M., Uggetti, E., Ferrer-Marti, L., Calderon, A., Velo, E., 2011. Biogas production in low-cost household digesters at the Peruvian Andes. Biomass & Bioenergy 35, 1668–1674.
Garfí, M., Ferrer-Martí, L., Perez, I., Flotats, X., Ferrer, I., 2011. Codigestion of cow and guinea pig manure in low-cost tubular digesters at high altitude. Ecological Engineering 37, 2066–2070.
Gautam, R., Baral, S., Heart, S., 2009. Biogas as a sustainable energy source in Nepal: present status and future challenges. Renewable and Sustainable Energy Reviews 13, 248–252.
Gebremedhin, K.G., Wu, B., Gooch, C., Wright, P., Inglis, S., 2005. Heat transfer model for plug-flow anaerobic digesters. Transactions of the Asae 48, 777–785.
Hashimoto, A.G., Chen, Y.R., 1979. The overall economics of anaerobic digestion. In: First International Symposium on Anaerobic Digestion, University College, Cardiff, Wales, England (September 17–21).
Hillel, D., 1982. Introduction to Soil Physics. Academic Press, San Diego, CA.
Hills, L.A., 1986. Analysis and optimum design of a methane digester for use on dairy farms. Unpublished M.S. Thesis. Department of Biological and Environmental Engineering, Cornell University, Ithaca, NY.
Incropera, F.P., DeWitt, D.P., 1996. Fundamentals of Heat and Mass Transfer, fourth ed. John Wiley & Sons, New York.
Kishore, V.V.N., 1989. A heat-transfer analysis of fixed-dome biogas plants. Biological Wastes 30, 199–215.
Lansing, S., Martin, J.F., Botero, R., Nogueira da Silva, T., Dias da Silva, E., 2010. Methane production in low-cost, unheated, plug-flow digesters treating swine manure and used cooking grease. Bioresource Technology 101, 4362–4370.
Liming, H., 2009. Financing rural renewable energy: a comparison between China and India. Renewable & Sustainable Energy Reviews 13, 1096–1103.
Martí-Herrero, J., 2007. Transfer of low-cost plastic biodigester technology at household level in Bolivia. Livestock Research for Rural Development 19(12) [cited May 2012]. Available from http://www.lrrd.org/lrrd19/12/mart19192.htm.

Martí-Herrero, J., 2008. Biodigestores Familiares: Guía de diseño y manual de instalación. La Paz, Bolivia, Cooperación Técnica Alemana-GTZ. ISBN: 978-99954-0-339-3. [cited May 2012]. Available from http://books.google.es/books?id=TsbrdcmKGKoC.

Martí-Herrero, J., 2011. Reduced hydraulic retention times in low-cost tubular digesters: two issues. Biomass and Bioenergy 35 (10), 4481–4484.

Martí-Herrero, J., Cipriano, J., 2012. Design methodology for low cost tubular digesters. Bioresource Technology 108, 21–27.

Perrigault, T., 2009. Mejoramiento del comportamiento térmico de un biodigestor low-cost tipo plug-flow. M.Sc. Thesis, Universitat Politècnica de Catalunya. Spain. [cited May 2012]. Available from http://upcommons.upc.edu/pfc/handle/2099.1/9229.

Poggio, D., 2007. Diseño y construcción de dos biodigestores en el altiplano peruano. M.Sc. Thesis, Universitat Politècnica de Catalunya. Spain. [cited May 2012]. Available from http://upcommons.upc.edu/pfc/handle/2099.1/4109.

Poggio, D., Ferrer, I., Batet, Ll., Velo, E., 2009. Adaptación de biodigestores tubulares de plástico a climas fríos. Livestock Research for Rural Development. 21 (9), 1-14. [cited May 2012]. Available from http://www.lrrd.org/lrrd21/9/pogg21152.htm.

Preston, T.R., Rodríguez, L., 2002. Low-cost biodigesters at the epicenter of ecological farming systems. Proceedings Biodigester Workshop, March 2002. [cited May 2012]. Available on http://www.mekarn.org/procbiod/prest.htm.

Ridley, B., Boland, J., Lauret, P., 2010. Modelling of diffuse solar fraction with multiple predictors. Renewable Energy 35, 478–483.

Sarwatt, S.V., Lekule, F.P., Preston, J.R., Dolberg, F., Petersen, P.H., 1995. On farm work with low cost tubular plastic biodigesters for resource poor farmers in Tanzania. In: Development Workers Conference. Dolberg, F., Novembervej, IJ Aarhus, Denmark.

Singh, D., Singh, K.K., Bansal, N.K., 1985. Heat loss reduction from the gas holder fixed gas dome of a community-size biogas plant. Energy Research 9, 417–430.

Swinbank, W.C., 1963. Long-wave radiation from clear skies. Quarterly Journal of the Royal Meteorological Society 89, 339.

Torres, J.L., De Blas, M., García, A., de Francisco, A., 2010. Comparative study of various models in estimating hourly diffuse solar irradiance. Renewable Energy 35, 1325–1332.

Usmani, J.A., Tiwari, G.N., Chandra, A., 1996. Performance characteristic of a greenhouse integrated biogas system. Energy Conversion and Management 37 (9), 1423–1433.

Velo, E., 2006. Aprovechamiento energético de la biomasa. In: Velo E., Sneij J., Delclòs J. (Eds.), Energía, participación y sostenibilidad. Tecnología para el desarrollo humano. Barcelona: Ingeniería Sin Fronteras – ISF. p. 131e44. [cited May 2012]. Available from http://grecdh.upc.edu/publicacions/llibres/documents/eps.pdf.

Weatherford, V., 2010. Verification of a thermal model for affordable solar-assisted biogas digesters in cold climates. M.Sc.Report. University of Colorado. USA.

Wu, J., Nofziger, D.L., 1999. Incorporating temperature effects on pesticide degradation into a management model. Journal of Environmental Quality 28, 92–100.

Yu, L., Yaoqiu, K., Ningsheng, H., Zhifeng, W., Lianzhong, X., 2008. Popularizing household-scale biogas digesters for rural sustainable energy development and greenhouse gas mitigation. Renewable Energy 33, 2027–2035.

Zhang, L., Yang, Z., Chen, B., Chen, G., 2009. Rural energy in China: pattern and policy. Renewable Energy 34, 2813–2823.